JACS
JOURNAL OF THE AMERICAN CHEMICAL SOCIETY

COMMUNICATION

pubs.acs.org/JACS

Plasmon-Mediated Photopolymerization Maps Plasmon Fields for Silver Nanoparticles

Kevin G. Stamplecoskie, Natalia L. Pacioni, Dayle Larson, and Juan C. Scaiano*

Department of Chemistry, Centre for Catalysis Research and Innovation, University of Ottawa, 10 Marie Curie, Ottawa, Ontario K1N 6N5, Canada

Supporting Information

ABSTRACT: Visible light exposure of films containing silver nanoparticles (AgNPs) shows that the enhanced field around AgNPs in a thin film containing an azo free radical initiator (AIBN) and a triacrylate selectively cross-links the triacrylate within the plasmonic region around the particles. The cross-linked polymer is less soluble than its precursor and behaves as a solubility switch. After the film is developed with ethanol, polymer-encapsulated nanoparticles are preserved on the surface. The 8−10 nm polymer structure that encapsulates the particles effectively maps and preserves the morphology of the plasmon field in AgNP-controlled nanostructures.

When excited in the plasmon region, metal nanoparticles have intense localized electromagnetic fields in the direct vicinity of the particles.[1] The plasmon fields that characterize noble metal nanoparticles can influence the spectroscopic and thermal behavior of molecules in close proximity (<20 nm) to the metal surface. Such effects can result in enhanced fluorescence,[2] surface-enhanced Raman signals (SERS),[3] and enhanced triplet formation,[4] as well as thermal processes characteristic of high-temperature behavior.[5,6] In a recent example, plasmon-assisted processes were used to release fluorophores by triggering retro-Diels−Alder chemistry.[7] In this Communication we explore the possibility of using plasmon-mediated chemistry to initiate polymerization processes that encapsulate particles in a way that effectively "maps" the plasmon field surrounding silver nanoparticles (AgNPs); we show that the enhanced field around AgNPs can be excited by nonpolarized light in a thin film containing AgNPs, an azo free radical initiator (2,2′-azo-bis-isobutyronitrile, AIBN), and a triacrylate. Plasmon excitation results in cross-linking of the triacrylate within the enhanced electromagnetic field around the AgNP. The cross-linked polymer is less soluble than its precursor and works as a negative image in which only the polymerized regions remain fixed to the film after washing with ethanol.

The choice of AgNP (rather than, e.g., AuNP or CuNP) deserves comment. The absorption coefficient of metal nanoparticles has an inverse relationship with the imaginary part of the dielectric constant, so smaller imaginary dielectric constants give rise to large absorption coefficients. Silver has the lowest dielectric constant among Ag, Au, and Cu at the corresponding resonance frequency, making Ag a great candidate for high absorption of visible light. When the surface plasmon absorption is excited, there is a resultant electromagnetic field around the particles that enhances the electronic transition of molecules in the direct vicinity of the particles.[8] The intensity of the electromagnetic field is related to conductivity, and

Chart 1. Chemical Structures of AIBN Used as an Initiator for Plasmon-Enhanced Polymerization and the Monomer, TMPTA, Used as an Efficient Cross-Linker

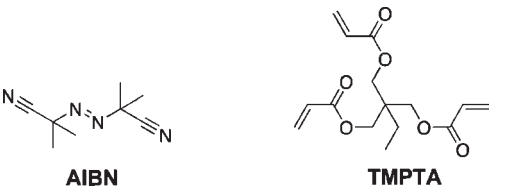

Ag is known to have the highest resultant electromagnetic field among these elements. Overall, Ag has a high absorption coefficient and a high resultant electromagnetic field enhancement when excited at ∼400 nm (for spherical nanoparticles), and it is this field that leads to an enhancement of electronic transitions in neighboring molecules, in our case an azo photoinitiator. It is noteworthy that Au generally has higher stability against oxidation, and it may be possible to have the same effect with Au, as what is described for Ag here. Ag is simply chosen for its superior photophysical properties for this application.

Our experiments have been performed using small AgNP seeds (∼3.3 nm) prepared photochemically,[9] followed by slow growth to achieve ∼40 nm particles using an ascorbic acid reduction process described in detail in the Supporting Information (SI). The average diameter of the particles as prepared was determined to be 38.3 nm (sd = 6.0 nm) by drop-casting onto a quartz plate and imaging by SEM. An azo compound (AIBN) was used as a free radical initiator and a triacrylate (trimethylolpropane triacrylate, TMPTA) as the monomer; these structures are shown in Chart 1. After several tests for compatibility of the various materials and the ability to produce good spin-coated films, acetonitrile was selected as casting solvent. The triacrylate used has the ability to cross-link extensively and thus produces rather insoluble polymeric structures, effectively acting as a solubility switch where polymerization occurs.[10]

The initiator, AIBN, is known to generate carbon-centered radicals either photochemically or thermally, in the latter case with an activation energy of 34.1 kcal/mol.[11] In our system we reasoned that plasmon-mediated excitation could promote AIBN decomposition in the vicinity of the AgNP and that this, in turn, would initiate localized polymerization. The films were produced by spin-coating (3500 rpm, 30 s) a solution containing 20 wt % TMPTA, 1 wt % AIBN, and >0.2% silver in the form of AgNP in

Received: February 20, 2011
Published: May 26, 2011

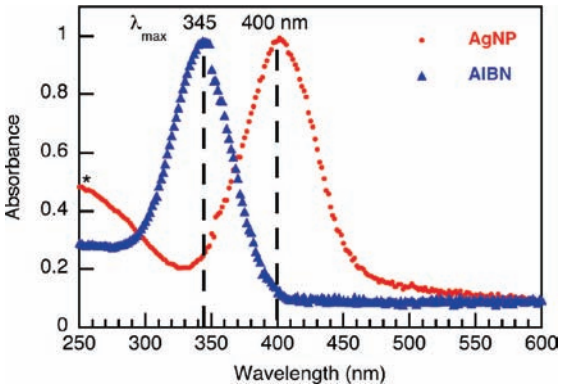

Figure 1. UV−vis absorption spectra of AIBN and AgNP. Normalized UV−vis absorption spectra of AIBN (blue) and AgNP (red) in acetonitrile, with dashed lines showing the position of the absorption maximum, especially highlighting the fact that AgNP can be excited at $\lambda > 400$ nm, where AIBN is transparent without plasmon enhancement. Note that the absorbance at 250 nm (marked *) for the AgNP solution is due to traces of products derived from the I-2959 photoinitiator used to reduce the Ag^+ salt while making AgNP.

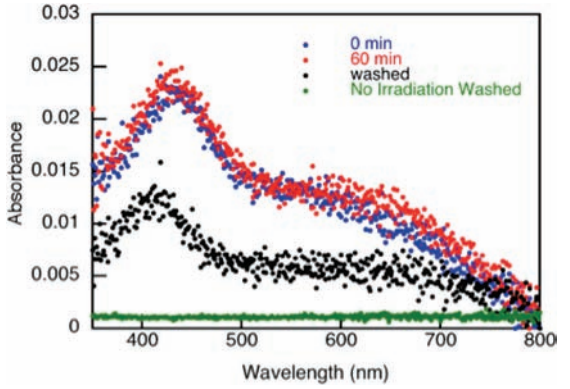

Figure 2. UV−vis absorption spectra of a film for plasmon-enhanced polymerization. UV−vis absorption spectra for a freshly prepared AgNP film (blue), a film irradiated with 405 nm light for 60 min (red), showing little change upon irradiation, the irradiated film after washing with ethanol (black), and a spectrum of a freshly prepared film that was washed without irradiation (green), showing that AgNPs do not persist on the films when washed with ethanol if they are not irradiated to induce plasmon-enhanced polymerization. The black spectrum has a residual absorption for AgNPs that have been "fixed" to the film by 405 nm excitation. Note that the absorbance values are very low (0.025 max), which also results in a poor signal/noise ratio, which is anticipated since the films are only 100 nm thick. An equivalent concentration of AgNP in a 1 × 1 cm cuvette would correspond to a nominal absorbance of 2500.

ACN/DMF. Typical film thickness was ∼100 nm, as determined by interferometry (see SI). Films were irradiated with a single 405 nm light-emitting diode (LED) with a light flux of ∼207 W/m^2. In principle, AIBN can also be decomposed by direct photolysis, but it is essentially transparent at 405 nm, the wavelength of the LED used for excitation. Figure 1 shows the corresponding spectra recorded in solution.

The effect of LED AgNP excitation on the film spectroscopy and dissolution is illustrated in Figure 2, and shows clearly that while exposure does not change the optical properties of the film, it dramatically changes its dissolution behavior. Thus, ethanol washing of the unexposed film totally removes the AgNP, as

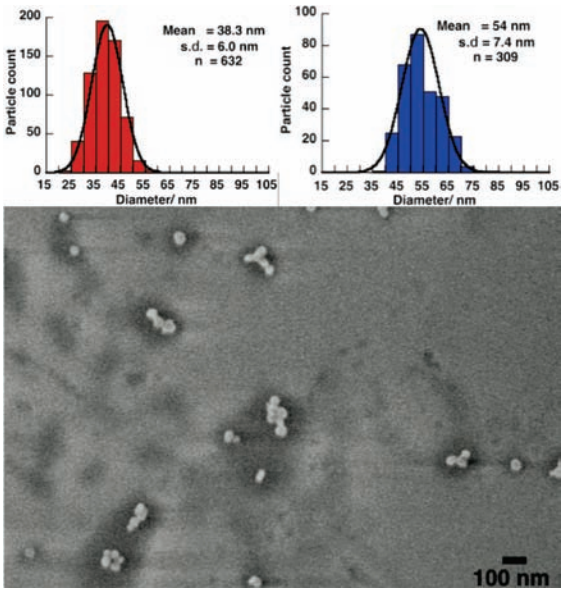

Figure 3. Histograms of AgNP size with and without polymerization and a representative SEM image of a polymerized AgNP film. Bottom: representative SEM image of AgNP after polymerization and washing with ethanol, showing the particles that remain on the film. Top: histograms of the AgNP sizes as measured from SEM images for particles drop-cast without monomer (red, left) and for particles after the polymerization and washing as in the SEM image (blue, right).

evidenced by the absence of the 400 nm plasmon band following ethanol treatment; in contrast, in the exposed film, about 50% of the AgNP absorption remains after ethanol treatment.

In order to establish if the observation of Figure 2 was a true indication of plasmon-localized phenomena, a series of experiments were performed using SEM and AFM imaging techniques. SEM demonstrated that AgNPs were retained on the surface; further, these particles were larger than those initially deposited, with an average size of 54 nm, compared with 38.3 nm initially, or a growth of approximately 16 nm, suggesting that a layer of ∼8 nm has been deposited on the AgNP (Figure 3).

We noted in the SEM data some indication that particles in pairs or groups had a higher probability of being preserved in the films. Our AFM data confirm this observation. Several images have been included in the SI, while Figure 4 illustrates particles with a clear two-particle definition. The measured size of the particles by SEM was larger for the polymerized particles, as stated above, and to confirm this finding the height of AgNPs from the polymerized films was compared with the height of drop-cast AgNPs (as determined from cross sections such as those in Figure 4). We note that the height determination was performed on a random selection of particles (all particles imaged in AFM) with and without polymerization, and no preference was given to measuring dimers, trimers, or any aggregates of AgNPs. The line scans are a measure of the AFM topography in a line that is assigned over the particles, whereby the particle height is measured as the maximum minus the minimum in the line scan and indicated by the arrows in the line scans of Figure 4. The AFM data are summarized in the SI, but it is worth noting here that the average height of the polymerized AgNP was 53.6 nm, compared to 44.9 nm for the original particles, indicating a ∼10 nm size increase upon polymerization.

dx.doi.org/10.1021/ja201139z |J. Am. Chem. Soc. 2011, 133, 9160–9163

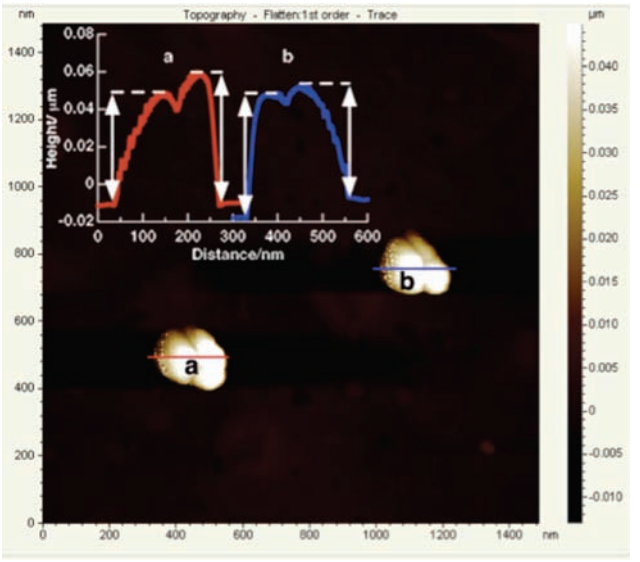

Figure 4. AFM image of a polymerized AgNP film. Main panel: representative topographic AFM image (scanning range 1.5 μm × 1.5 μm) of AgNPs after plasmon-enhanced polymerization and ethanol washing. Inset graphs: height profiles taken for two separate clusters of AgNP on the film. The height of AgNP by AFM was determined as the difference between the maximum/minimum of the cross section, as indicated by the arrows.

The AFM images reveal that polymer-coated particles have remained on the surface and that no polymer debris is observed in regions free from AgNP. Further, many particles are frequently in pairs or groups—many more than observed in nonpolymerized drop-cast samples—as already noted for the SEM data. Interestingly, the particles seem to grow (based on AFM height) about 10 nm, similar to the observation by SEM. We speculate that growth occurs on both sides of the particle in the x and y directions, while in the vertical or z direction growth occurs only above the particle, with little or no growth in the contact area between the substrate and the particle. XPS measurements (see SI) show that there is a significant amount of carbon on the polymerized films even after washing with ethanol, as expected. Also, upon Ar-ion etching to remove the polymer, the carbon content decreases, and there is a small enhancement in the exposed Ag detected by XPS, which is consistent with the prediction that the polymer is coating the AgNP from the plasmon-directed polymerization process.

The results presented in this Communication demonstrate that it is possible to take advantage of localized plasmon fields to trigger spatially controlled chemical reactions in molecules that are not chemically bound to the surface; quite simply, the intense electromagnetic field in the immediate vicinity of the particle(s) selects the molecules for reaction. The LED 405 nm light was specifically chosen to excite the maximum absorption for spherical AgNP while avoiding excitation of AIBN that is not in the near vicinity of the particles. It is the plasmon-induced excitation of AIBN near AgNP that causes initiation of polymerization by photodegradation of AIBN and, therefore, selective cross-linking of the monomer only in the enhancement region. The formation of a highly insoluble cross-linked vinyl polymer acts as a solubility switch; further, these processes remain delicately confined to a well-defined region controlled by the plasmon field. Interestingly, it has been reported that the 2-cyano-2-propyl radical from AIBN shows transient binding to gold nanoparticles;[12] if a similar effect occurs with AgNP, this may assist to retain the geometric definition of the plasmon-intensified region as the polymerization occurs. The polymeric features observed are 8−10 nm in dimension, and are obtained with noncoherent 405 nm low-intensity excitation, and are over an order of magnitude smaller than achievable by diffraction-limited processes. Further, SERS and nanoantenna studies suggest that plasmon fields are greatly intensified in the interparticle regions,[13,14] a property that has been utilized to advantage in the design of antennas.[15] The apparent preference for particle aggregates of a few particles suggests that plasmon-mediated polymerization follows similar preferences. Of course, irradiation does not cause aggregation of particles in the films, but rather that the particles on the films that randomly exist in close proximity have very intense EM field intensities between them that cause intense polymerization in these highly enhanced regions. Therefore, these particles have a higher probability of inducing significant cross-linking in the interparticle space, and thus a higher probability of being retained on the films. This suggests that the effect is electronic rather than thermal.[6,7] The same has been observed in nanogaps designed with top-down strategies.[14] Further, from the statistical analysis of the AFM and SEM data (see SI), the standard deviation (sd) values, as an estimate of the variance of the population (s^2) in the heights and diameters, are different for drop-cast versus polymerized films.

While our work has taken advantage of random particle positioning resulting from the coating process, the results suggest that nanostructures in masks with well-defined geometric arrays could be used as plasmonic templates to generate custom lithographic features with a resolution of a few nanometers, potentially extending the lithographic limits well beyond those achievable with current top-down lithographic technologies. Thus, bottom-up self-assembly in the synthesis of nanostructures and in the polymerization stage could be combined with top-down mask design to achieve high resolution. Our work shows that plasmonic fields can be mapped and preserved by taking advantage of enhanced fields to initiate chemical processes capable of converting transient fields into permanent nanostructures.

■ ASSOCIATED CONTENT

Supporting Information. Synthesis details, particle growth mechanism, film preparation, exposure and plasmon polymerzation, statistical analysis, XPS analysis, and additional AFM and SEM images. This material is available free of charge via the Internet at http://pubs.acs.org.

■ AUTHOR INFORMATION

Corresponding Author
tito@photo.chem.uottawa.ca

■ ACKNOWLEDGMENT

We thank the Natural Sciences and Engineering Research Council for generous financial support.

■ REFERENCES

(1) Moores, A.; Goettmann, F. *New J. Chem.* **2006**, *30*, 1121–1132.
(2) Anger, P.; Bharadwaj, P.; Novotny, L. *Phys. Rev. Lett.* **2006**, *96*, 113002.
(3) Aroca, R. *Surface-Enhanced Vibrational Spectroscopy*; Wiley: Chichester, 2006. Stamplecoskie, K. G.; Scaiano, J. C.; Tiwari, V. S.; Anis, H. *J. Phys. Chem. C* **2011**, *105*, 1403–1409.

(4) Pacioni, N. L.; González-Béjar, M.; Alarcón, E.; McGilvray, K. L.; Scaiano, J. C. *J. Am. Chem. Soc.* **2010**, *132*, 6298–6299.
(5) Adleman, J. R.; Boyd, D. A.; Goodwin, D. G.; Psaltis, D. *Nano Lett.* **2009**, *9*, 4417–4423.
(6) Fasciani, C.; Alejo, C. J. B.; Grenier, M.; Netto-Ferreira, J. C.; Scaiano, J. C. *Org. Lett.* **2011**, *13*, 204–207.
(7) Bakhtiari, A. B. S.; Hsiao, D.; Jin, G.; Gates, B. D.; Branda, N. R. *Angew. Chem., Int. Ed.* **2009**, *48*, 4166–4169.
(8) Nabika, H.; Takase, M.; Nagasawa, F.; Murakoshi, K. *J. Phys. Chem. Lett.* **2010**, *1*, 2470–2487. Schuller, J. A.; Barnard, E. S.; Cai, W.; Jun, Y. C.; White, J. S.; Brongersma, M. L. *Nat. Mater.* **2010**, *9*, 193–204.
(9) Stamplecoskie, K. G.; Scaiano, J. C. *J. Am. Chem. Soc.* **2010**, *132*, 1825–1827. McGilvray, K. L.; Decan, M. R.; Wang, D.; Scaiano, J. C. *J. Am. Chem. Soc.* **2006**, *128*, 15980–15981.
(10) Uzum, O.; Karadag, E. *Polym. Plast. Technol.* **2010**, *49*, 9609–9616. Hageman, H. J.; Jansen, L. G. J. *Makromol.Chem.* **1988**, *189*, 2781–2795.
(11) Aspee, A.; Garcia, O.; Maretti, L.; Sastre, R.; Scaiano, J. *Macromolecules* **2003**, *36*, 3550–3556.
(12) Aprile, C.; Corma, A.; Domine, M. E.; Garcia, H.; Mitchell, C. *J. Catal.* **2009**, *264*, 44–53.
(13) Zou, S.; Schatz, G. C. *Chem. Phys. Lett.* **2005**, *403*, 62–67.
(14) Ueno, K.; Takabatake, S.; Nishijima, Y.; Mizeikis, V.; Yokota, Y.; Misawa, H. *J. Phys. Chem. Lett.* **2010**, *1*, 657–662.
(15) Farcau, C.; Astilean, S. *J. Phys. Chem. C* **2010**, *114*, 15266–15273. Sundaramurthy, A.; Schuck, P. J.; Conley, N. R.; Fromm, D. P.; Kino, G. S.; Moerner, W. E. *Nano Lett.* **2006**, *6*, 355–360.